Contributions to Geophysics and Geodesy Vol. 54/4, 2024 (345–369)

Application of seismic refraction tomography for determining ground water potential zone in the Qularaisi area, Sulaimaniyah city, NE Iraq

Abdulla K. AMIN[1,*], Kwestan M. AHMED[2], Ezzadin N. BABAN[3]

[1] Department of Social Sciences, College of Basic Education, University of Sulaimani, Sulaimani, Iraq; e-mail: Abdullakarim2004@gmail.com

[2] Ground water Directorate Sulaimani, Sulaimani, Iraq; e-mail: kwestan.muhamad2022@gmail.com

[3] Department of Geology, College of Science, University of Sulaimani, Sulaimani, Iraq; e-mail: Ezadin@gmail.com

Abstract: Delineating zones with the potential groundwater contains is a crucial for the effective exploration and extraction of this resource. Six seismic refraction traverses for measuring compressional wave velocities (v_p) were conducted in the Qularaisi area, northwest of Sulaimaniyah City in the Kurdistan Region of Iraq to determine the ground water potential zone in the selected area, each traverse has a total length of 230 m, with an inter-geophone spacing of 5 m. The velocities and the thickness of each layer were subsequently calculated based on the obtained data. This analysis provides insights into the geological formation and composition of the area. The interpretation results reveal the presence of three distinct geological layers. The first upper layer consists of clay topsoil deposits characterized by brittle materials, with the thickness ranging from 0 to 4.2 m and seismic velocities (v_p) between 339 and 583 m/s. The second layer, with a thickness of 4.2 to 16.8 m and v_p values between 1248 and 2650 m/s, corresponds to recent deposits of clay, sand, silt, and gravel, interpreted as unconsolidated sediments. The third layer is characterized as a consolidated marly limestone belonging from the middle Tanjero formation, occurring at depths exceeding 20 metres. This layer reflects a more compact geological structure, distinguishing it from the overlying unconsolidated materials with the v_p values ranging from 3606 to 4844 m/s. The seismic refraction results indicate that the aquifer is a sand and gravel inter-granular aquifer at the depth to the saturated groundwater layers in the area ranges from 10 to 25 m whereas lower layer of marl bed reaches to a depth of 40.2 m acts as the impermeable bed.

Key words: seismic refraction tomography, primary wave velocity, ground water, Seis-Imager/2D

*corresponding author, e-mail: Abdullakarim2004@gmail.com

doi: 10.31577/congeo.2024.54.4.3

1. Introduction

Ground water resources are more important for the public water supply than surface water, more ever global spend of the surface water due to population increasing, global warming and draught will lead to decreasing of its quantity and subjected to contamination and pollution when compared to the ground water. Many environmental problems directly or indirectly related to the location of ground water and its protection from contamination sources of various kinds with a rapid increase in population and growth of industrialization, ground water quality is being increasingly threatened by the disposal of urban and industrial solid waste (*Janardhana Raju et al., 2011; Singh et al., 2015*).

Many geophysical methods are commonly applied to investigate ground water through applying different geophysical equipment's for detecting ground water in any hydrogeological study such as Seismic Refraction Tomography (SRT), Electrical Resistivity Tomography (ERT), gravity and magnetic as well as seismic refraction methods were used to map regional aquifers and large-scale basin features (*Mota, 1954; Haeni, 1988*). These methods are also used in foundation studies, civil engineering projects, siting studies, engineering environmental, geotechnical investigations, ground water, dam safety analyses and tunnel alignment studies (*Lankston 1989; Hodgkinson and Brown, 2005; Bridle, 2006; Yilmaz et al., 2006*).

The refraction method is widely used for the characterization of ground water depth. In particular case, in porous soils of the unsaturated as well as saturated interface by a refracting surface, efficaciously detected by the mentioned exploration method (*Haeni, 1988*).

Sharafeldin (2008) applied a 2D-seismic refraction survey, performed to study the bedrock conditions of a proposed dam and reservoir site in Wadi Asala, Jeddah area, Saudi Arabia. *Uyanık (2011)* suggested that several factors affect seismic velocities through soils and rocks including lithological, physical and elastic properties of soils. *Mirassi and Rahnema (2020)* applied propagation of seismic waves in homogenous half-space and layered soil media for Deep cavity detection. *Desper et al. (2015)* used the refraction method to estimate water table depth in a shallow unconfined aquifer in the Mulgrave River basin (Australia).

Dhamiry and Zouaghi (2020) applied near-surface geophysical surveys such as, seismic refraction tomography (SRT) The geophysical surveys high-

light the vertical and lateral distribution of the ground velocity and resistivity parameters at marine Yanbu port in Yanbu province, western Saudia Arabia for the purpose of mapping the depth of the bedrock and defining stratigraphic type and thickness of the overlying sediments.

Besides, integration between two or more geophysical methods had been very successful to detect the subsurface layers and features and reduce the uncertainty caused by a single geophysical method (*Gao et al., 2018; Loperte et al. 2016; Samyn et al., 2014*).

This site was chosen due to the rare geophysical studies in the area and it is surrounding, especially the seismic refraction method, which as yet there is no previous study and also the existence of other verification tools such as outcrops and boreholes data information which is always helpful in interpreting data. In addition, this area is located around the city centre close to a place of residence and will eventually be a residential area shortly leading to increasing demands on the water as a result of rapid population increases, this shows the importance and effect of geophysical methods in ground water investigation in this area without costing too much and detecting subsurface layers including aquifer layer with its depth and thickness and reveal the hydraulic gradient of the area and appearing ground water movement and accumulate in the aquifer.

2. Location of the studied area

The study area is located in the Qularaisi area of NW Sulaimaniyah city, Kurdistan Region – Iraq. Geographically, the studied area lies in the zone of 38S occupying an area of 108,000 m^2 its latitudes and longitudes are shown on the map, as illustrated in Fig. 1.

3. Topography and geological setting

3.1. Topography

Topographically, the studied area is located in a flat area with small undulation is bounded by abroad mountainous region with Azmir and Goizha mountains covering the northeastern part of the area, whereas the height ranges between 1696 m and 1512 m above sea level (a.s.l) and the plunge of Sulaimani Anticline (Extension from the big Piramagrun Mountain). Al-

Fig. 1. Location map of the study area (*Google Earth, 2022*).

most 23% of the area is considered a mountainous region, which comprises Piramagrun, Azmir-Goizha, Sulaimani anticlines and Baranan Homocline, while central, and southern parts of the area, which represent about 77%, are a gently dipping flat terrain. The area is covered by alluvial plain deposits, which are gravels, pebbles, sandy and sandy silt mixed with clay of the Quaternary period (*Stevanovic and Markovic, 2003*). The top soil layer represents an enrichment agricultural plain area, which contains the most essential elements and is bounded by several mountains extending with the same trend of Zagros Mountain belts (NW–SE). In summary, the study area is located near the south of Shahin city, north of the Qularaisi-Sulaimani road, which is an approximately flat fertilizing agricultural area with small undulation. The maximum elevation in the area is about 827 m (a.s.l.) and the minimum values are nearly 805 m (a.s.l).

3.2. Geologic setting

The area consists of different geological formations from early Cretaceous to Quaternary age (*Karim and Ali, 2004; Sissakian and Fouad, 2015; Omar et al., 2015*), geological cross-section in Fig. 2. The Cretaceous formations in the area from the oldest to younger rocks are Balambo, Qamchuqa,

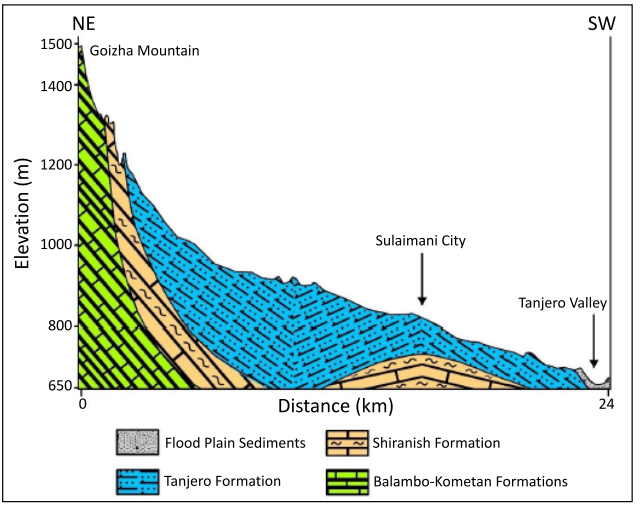

Fig. 2. Geological cross-section modified after (*Kareem et al., 2018*).

Kometan, Shiranish, and Tanjero formations. The Tertiary geological formations in the area are Kolosh, Sinjar, Gercus and PilaSpi formations. The Quaternary deposits generally consist of alluvial fans and flood plain sediments.

The age of these units' ranges from lower Cretaceous to Quaternary deposits, the oldest rocks are cropping out in the crest of anticlines in the Balambo formation, belonging to the Valanginian–Turonian age, whereas the younger units exposed along with the anticline limbs and in the trough of synclines. The selected area is located in the Quaternary deposits and Tanjero formation.

The Tanjero formation is widespread in the Sulaimani-Warmawa Subbasin, especially around the city of Sulaimaniyah, and extends from the foothills of Goizha Mountain in the north and northeast towards the Tanjero valley in the south and the Chaq-Chaq valley in the northwest (*Mustafa, 2006*). It is composed of silty marl, siltstone, shale, sandstone, conglomerate, and sandy or silty organic detrital limestone (*van Bellen et al., 1959*). Tanjero formation lies under the Quaternary deposits in the study area (Fig. 3).

The Tanjero formation divided into three parts based on its lithological composition, i.e., Lower, Middle and Upper part (*Karim and Ali, 2004*).

The lower part is mostly composed of the alteration of thin sandstone sliced between thick dark grey calcareous shale with transition to a thick bed of boulder and coarse gravel conglomerate beds. The middle part consists of bluish marl and the upper part is composed of mixed siliciclastic-carbonated beds represented as the alteration of thick-beds biogenic limestone, and calcareous shale on the shelf. Quaternary deposits are covering a wide part of the studied area are mostly composed of gravel, sand, silt, mud, sandy, and silty clay soil (*Mustafa, 2006; Sissakian and Fouad, 2015*).

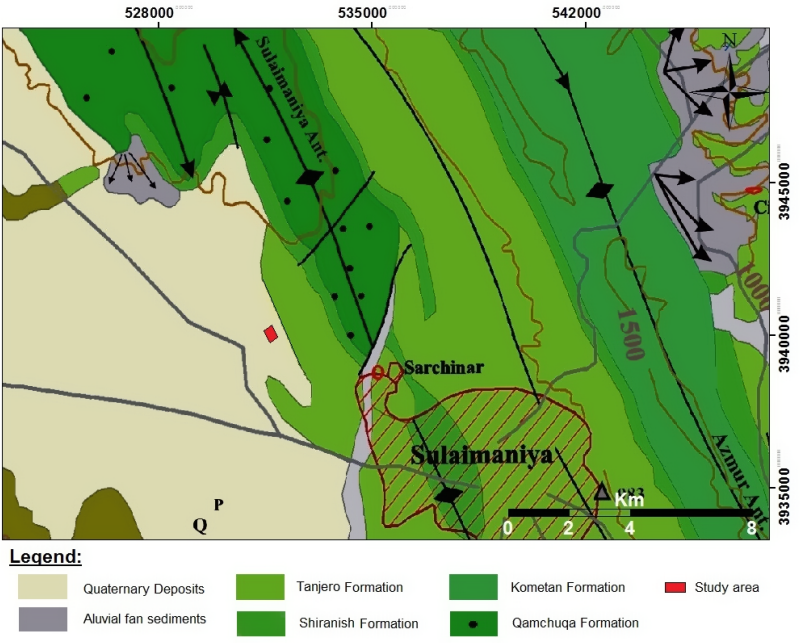

Fig. 3. Geological map of the study area (modified from *Ma'ala, 2008*).

3.3. Hydrology and hydrogeology of the studied area

Hydrologically, the study area is part of the Sulaimani-Warmawa sub-basin, which is bordered by two main sub-watersheds. The Chaqchaq sub-watershed is located approximately 3 km to the northeast of the study area, while the Kani-pan sub-watershed lies about 9.5 km to the southwest. The confluence of the Chaqchaq and Kani-pan streams forms the Tanjero River

near Kani Goma village. These streams, along with numerous smaller ones, create a dendritic drainage pattern.

According to *Moore (2002)* geologic conditions (types and sequence of rocks) in the subsurface have major control over the direction and quantity of ground water flow. However, according to *Hassan (1998); Chnaray (2003)*, the ground water flow direction is dependent on hydraulic conductivity (K) and hydraulic gradients. The water table also varies in depth according to local topography and prevailing climate (*Otutu, 2010*). For the current study, the ground water flow pattern map was constructed based on the data from 26 wells drilled in the surrounding area. The general flow direction of groundwater is from the northeast to the southwest, which corresponds to the area's topography. The ground water flow pattern is presented in Fig. 4. Generally, the hydro-stratigraphic units in Sulaimaniyah City have been grouped according to their lithology and hydrogeology characteristics into the Karstic Fissured aquifer, the Kometan aquifer, the Tanjero aquifer, an Aquiclude and a Quaternary intergranular aquifer (*Stevanovic and Markovic, 2003; Mustafa, 2006; Ali, 2007*).

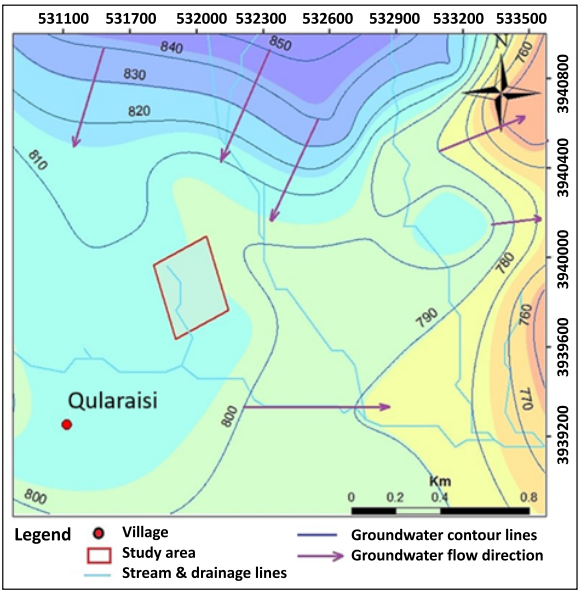

Fig. 4. Ground water flow pattern and drainage lines map within the study area.

According to the hydrogeological data and reports from the Sulaimani Directorate of Groundwater, the area is characterized by the presence of three distinct aquifers, which are Kometan and Tanjero formations aquifer and Shallow Quaternary aquifer with 0 – 25 m depth represents as a good and widespread aquifer in Sulaimaniyah City, which mostly includes alluvial fan sediments and in the southern part of the city floodplain sediments. The aquifer is composed of unconsolidated gravel, sand, silt, and clay that yield a good quantity of water (inter granular aquifer). In certain parts of the city, the aquifer is recharged and retains water exclusively during the wet seasons, with limited or no water availability during drier periods (*Mustafa, 2006*). From the hydrogeological point of view, the expected ground water is attributed to subsurface geological conditions, which reflect the presence of shallow to medium aquifer related to recent alluvium and Tanjero formation.

4. Topography

4.1. Fieldwork

The modern computerized instrument the Geode Exploration Seismograph was used to conduct field measurements. The Geode is a highly portable stand-alone distributed seismic module a with versatile and flexible seismograph, it is small and light weighting only 6 to 9 pounds enough to pack into your suitcase, yet easily expandable if needed for full-scale 2D and 3D surveys via our intelligently designed distributed architecture. Geode can be used for reflection, refraction, MASW/MAM, or tomography surveys. Additionally, it can be applied to various scenarios such as earthquake detection, quarry blast analysis, or monitoring heavy machinery operations.

In order to cover the study area, the seismic refraction survey was conducted along six traverses trending parallel to the strike direction. Each traverse consisted of two lines (A and B), each measuring 115 metres in length, with an inter-traverse spacing ranging from 15 to 75 m. The total length of each traverse is 230 metres, as illustrated in Fig. 5. The record length of P-waves was 0.250 sec with a sample interval of 62.500 μsec. For each P-wave shot location, three separate stacks were generated to enhance the signal-to-noise ratio because the study area is located near many noise sources such as traffic, daily human activities, machinery, and other factors.

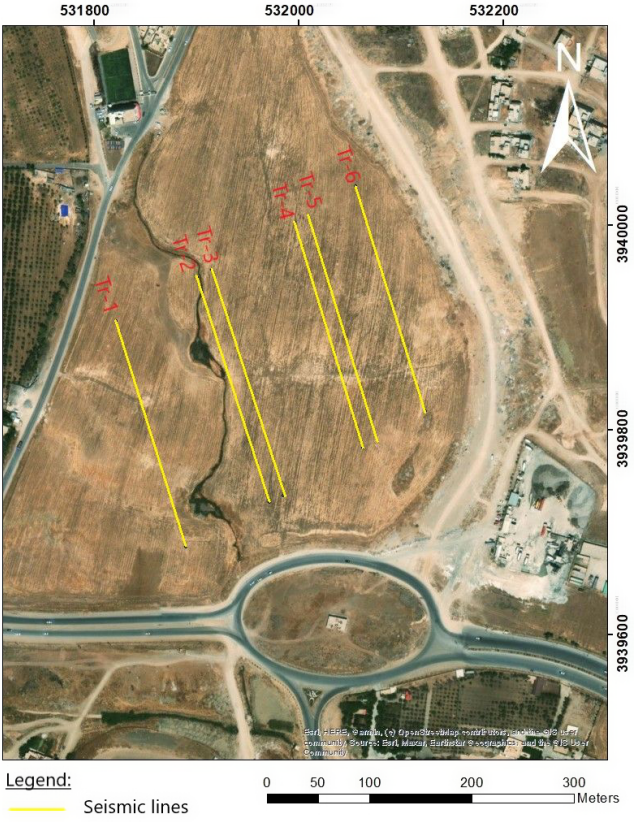

Fig. 5. Six traverses for SRT method in study location (*Google Earth, 2022*).

The coordinates of the traverses are presented in Table 1.

Table 1. Shows numbers, and coordinates of seismic survey traverses.

Traverses	South coordinates (end)		North coordinates (start)	
	East	North	East	North
Tr-1	531890	3939686	531822	3939907
Tr-2	531972	3939730	531901	3939950
Tr-3	531985	3939736	531915	3939957
Tr-4	532063	3939783	531996	3940004
Tr-5	532074	3939789	532004	3940009
Tr-6	532124	3939819	532056	3940039

4.2. Data acquisition

Seismic fieldwork is a crucial phase of any seismic survey that requires careful execution with high accuracy, as errors in measurements can affect subsequent phases. Before starting fieldwork, it is essential to consider site selection, survey objectives, geological information, expected seismic velocity contrasts, survey type (2D or 3D), number of traverses, geophone layout and spacing, and the energy source used... etc., *Reynolds (2011)*.

Field data acquisition, processing, and interpretation of seismic refraction data are usually fast, simple, and low-cost. Data acquisition involves generating seismic energy at several locations both within and around the spread of receivers.

Field survey measurements were carried out in the study area, where a total of 24 geophones were fixed on the ground surface and connected with seismic land cables with a total of 24 take outs was connected to the seismographs. Seismic shots were generated using a sledgehammer along the profile. Six seismic lines were carried out in the study area, each traverse consisting of two lines with a total length of 230 metres, as illustrated in Fig. 6.

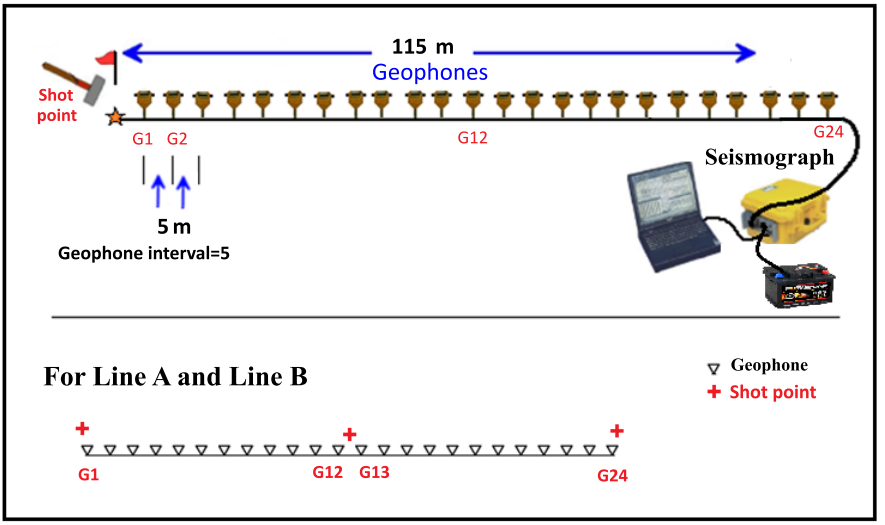

Fig. 6. A schematic diagram of the geometry of seismic survey.

5. Data processing

The processing and interpretation of acquired Seismic Refraction Tomography (SRT) data was carried out using the commercial software package (*Geometrics, 2021*, SeisImager/2D software), the software is composed of five packages but the Pickwin and the Plotrefa are the most relevant to this study. The first step of seismic data processing is to pick the first arrival times of seismic waves for each trace. By using Pickwin program to select the first arrival accurately or the first breaks for every shot record to obtain time-distance curves (*Dobrin and Savit, 1988; Haeni, 1986*). The time-distance curves were constructed based on the distance along the survey line, after picking the first breaks for all the seismic events, which are shown in Fig. 7.

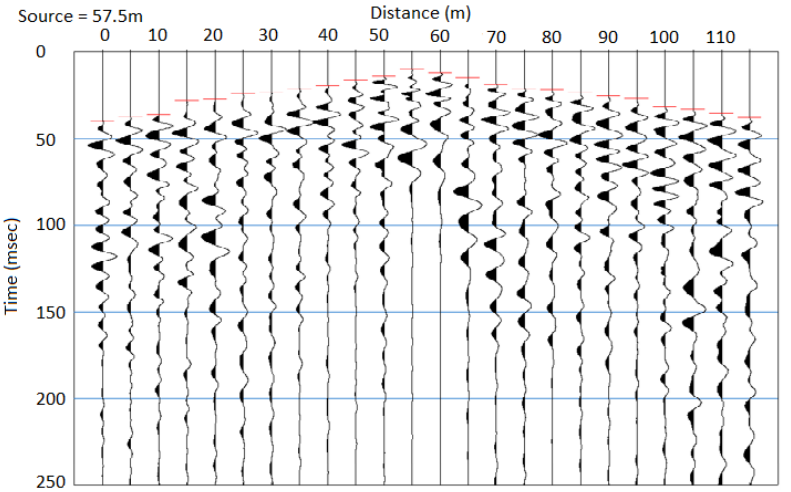

Fig. 7. Sample of seismic data after picking in the study area of Travers 5 after processing.

The following steps for data processing are applied; editing the geometry information in the header (trace headers) to reflect that of the actual survey by edit source and receiver location of the file. This is done by detect the longitude, latitude, and elevation of each shot point and geophone by using the GPS.

In software like Pickwin, which is used for seismic data processing, DC removal typically involves subtracting the mean value of the signal from

the entire dataset or applying high-pass filters to focus on the frequency components of interest. To accomplish the precise first arrival picking, the amplitude of each trace mutes the bad traces (noisy channels, poorly planted geophones, channels contaminated by power line noise, etc), as shown in Fig. 8. Then the result was saved in a file having an extension of "`.vs`". The data quality was improved using a bandwidth filter, which helped to more easily identify the first arrival signals for manual picking. The frequency cut-off filter was used to remove lower-frequency noise (below 38 Hz) and higher-frequency noise (above 80 Hz) from the raw data (*Geometrics, 2021*).

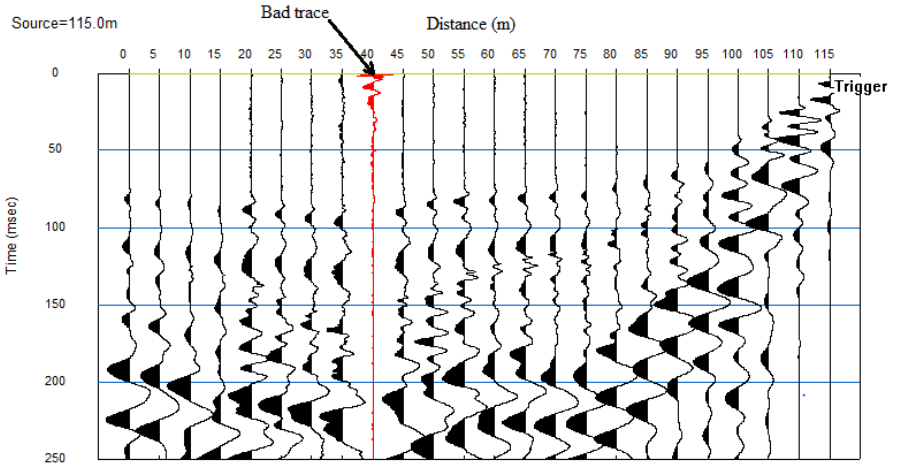

Fig. 8. A seismic record from Travers 4, after Avoiding DC offset.

The Plotrefa program was used in the second step for the interpretation refraction data. This program was used to explain the velocity model and layered model for the study area. This package was used to carry out the time-term inversion in order to generate the 2-D seismic section of the surveyed area. This inversion employs a combination of linear least squares and delays time analysis to invert the first arrival for a velocity section. The interpretation of seismic refraction data is done by the modelling and inversion of the acquired seismic velocities. Those velocities are determined from the travel-time plot for each seismic line by modelling the paths taken through the subsurface by the seismic energy.

The third step is modelling velocity-depth profiles from the observed seismic velocity by a tomographic inversion method provided by the Plotrefa

program. This method starts with an initial velocity model and iteratively traces rays through the model with the goal of minimizing the RMS error between the observed and calculated travel times. The observed and calculated data have a difference of RMS error of less than 4% and the low RMS error value indicated the best fit between the observed and calculated travel times. Finally, they inverted travel time data to a two-dimensional velocity section, which were represented in 2D images. This model converts the tomogram to a layered model to better represent the layered nature of geology. The results were saved in a file in an ASCII columnar XYZ format or text format for import into graphics programs such as Golden Grapher or Surfer software.

6. Interpretation of the results

6.1. Traverse Tr-1

The picking of the first arrival time of P-wave and Travel time (Time–Distance) curve of Tr-1 is shown in (Fig. 9a and b). The automated and manual picking of the first break arrival (red dashes line) is the first stage of processing for seismic record data that involves accurate picking of the first breaks from the seismic signal by using the Pickwin program for every shot record to obtain time-distance curves.

The 2D seismic refraction tomography showed the lateral and vertical distribution of the geologic layers (Fig. 10a,b,c). The inversion model of this traverse (Fig. 10b) shows several layers and sub-layer within the three distinct layers. The first layer, represented by pink and red colours, corresponds to the topsoil, with a thickness ranging from 0 to 3 m. This layer is relatively flat, exhibiting minor undulations. The second layer (yellow, and light green "yellows green" colours sub-layer models, and dark green) is composed of rock fragment (clay, sand, silt, and gravel), several lateral variations change along the layers, especially at the distance between 20–60 m, where an uplift is noticeable on the right-hand side.

The third layer features a generally irregular surface, located at a depth of 15.28 m. The surface of this layer, (dark blue colours) represents the top of the middle Tanjero formation. The upper portion of the Tanjero formation has been completely eroded due to the effects of weathering processes (*Karim and Ali, 2004*). In certain areas, depressions are filled with

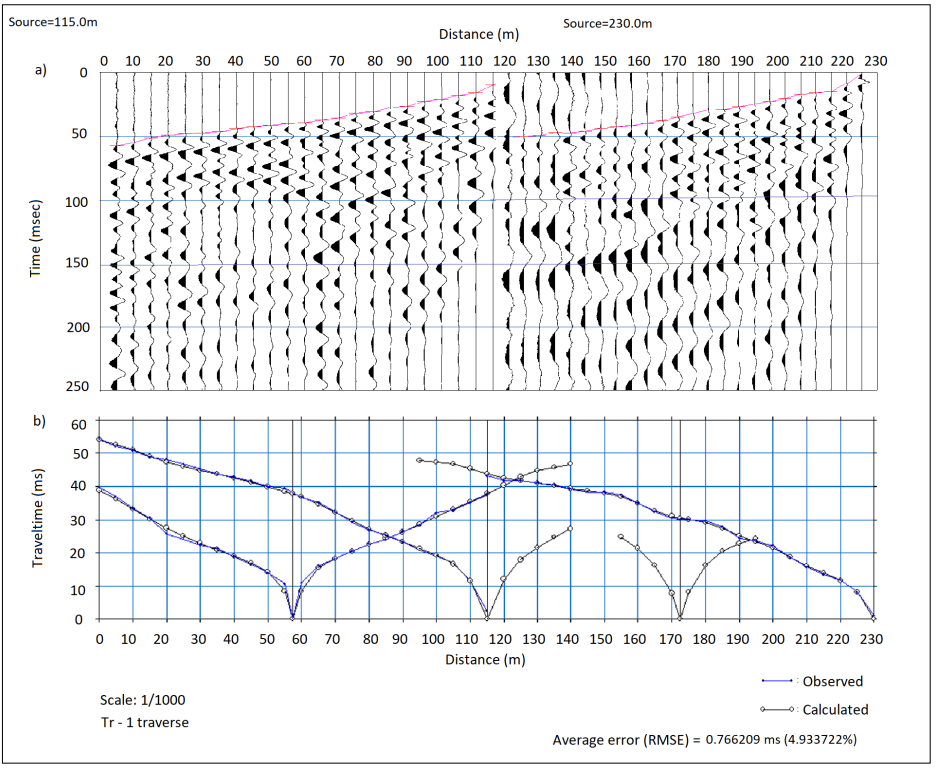

Fig. 9. Seismograph records a) first break picking, and b) P-wave travel time (Time–Distance) curve of Tr-1 traverse.

sediments from recent deposits resulting from erosion – the fourth sub-layer (light green colour). An uplift is observed in the fifth sub-layer (green colour) between distances of 30–60 m at an elevation of 809 m, and between 110–140 m at an elevation of 805 m. The sixth sub-layer, depicted in dark green, exhibits minor undulations. The seventh sub-layer (dark blue) reveals lateral variations, which may indicate paleo-erosional features. The eighth sub-layer, shown in blue, represents the solid and compact marl bed of the Tanjero formation. The surface of the Tanjero formation has undergone natural erosion beneath the weathered zone.

Figure 10c displays the three layer models for the 2-D seismic velocity section that was generated according to the lithological changes underneath the study area. The results indicate that a subsurface layer consists of three

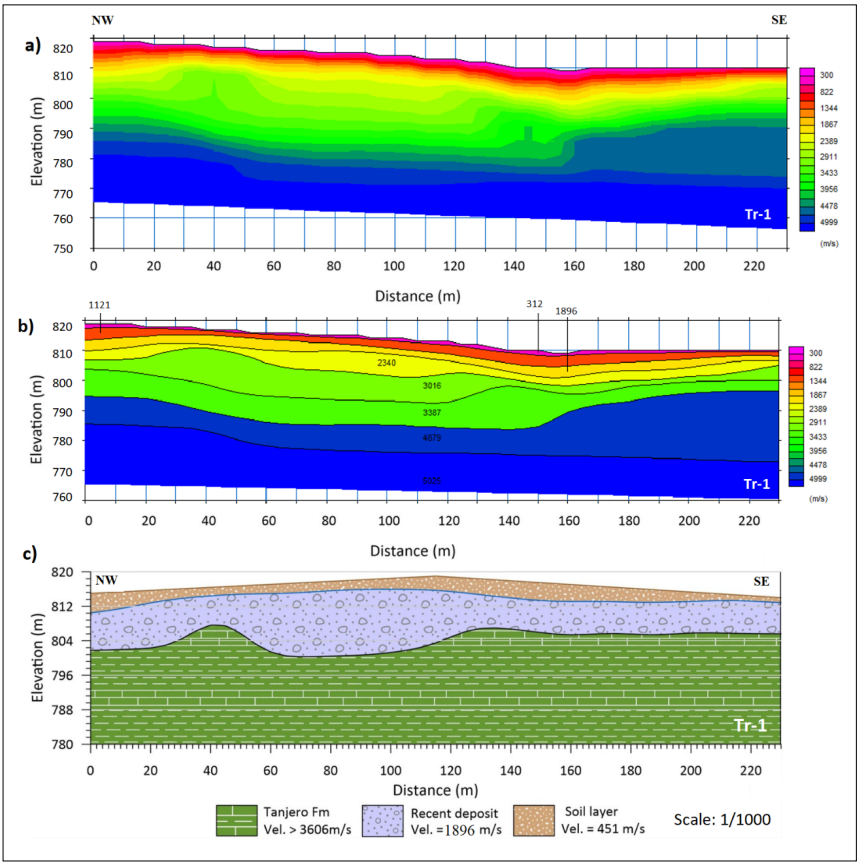

Fig. 10. SRT of traverse Tr-1; a) seismic refraction tomography (SRT) section, b) velocity model of the subsurface layers result from tomography, and c) the 2D velocity layer model and cross-section of the subsurface layers result from tomography inversion.

seismic layers with the velocity of each layer increasing with depth. This interpretation is supported by data from boreholes, outcrop information, and the local geology of the study site. The topmost layer is unconsolidated, with P-wave velocities ranging from 300 to 700 m/s and an average velocity of 451 m/s. The thickness of this layer varies between 0 and 2.78 m, and corresponds to the clay topsoil deposits. The second layer is semi-consolidated, composed of rock fragments, and exhibits velocities between 1867 and 2650 m/s, with an average velocity of 1896 m/s. The thickness of

this layer ranges from 2.78 to 12.5 m.

The velocities of these two layers show that the overburden layers consist of unconsolidated that was Recent deposits (clay, sand, silt, and gravel). Furthermore, the range velocity of these layers might be interpreted due to increasing water level presence (high water-saturated zone), according to the following relation of primary velocity (v_p) with the density (ρ):

$$v_p = \sqrt{\frac{B + \frac{4}{3}\mu}{\rho}},$$

where v_p is compressional wave velocity, B is bulk modulus, μ is shear modulus of material (axial modulus) and ρ is a density of material (*Kearey et al., 2002*).

An initial comparison between the p-waves and the aquifer layers highlights values ranging from 1200 to 1400 m/s in accordance with the results of *Hasselström (1969)* and *Haeni (1986)*.

The third layer, characterized as a consolidated layer, exhibits high seismic velocities ranging from 3433 to 4217 m/s, with an average velocity of 3606 m/s. This layer extends to a depth range of 3 to 15.28 m, reflecting its more compact and solid nature compared to the overlying layers. This layer corresponded to the middle part of the Tanjero formation which is mostly composed of marl layers causing an obvious increase in seismic velocity. Generally, the topography of the Tanjero formation has lateral variation change due to weathered probably caused by collapse or subsidence which is filled by sediment deposits.

6.2. Traverses Tr-2 and Tr-3

The sub-surface layers change with increasing depth (Fig. 11a,b,c) shows the 2D seismic section (SRT).

The inversion model of this traverse (Fig. 11b) shows that the first layer (pink, and red colour) represents to soil cover, with a thickness of 3.4 m. The second layer, representing rock fragments such as clay, sand, silt, and gravel, is shown with an elevation of 792 m (dark green colour), marking the top of the weathered middle Tanjero formation. In some areas, this layer is filled with recent sediment deposits. The third layer, illustrated in light blue, represents the Tanjero formation, characterized by minor undulations.

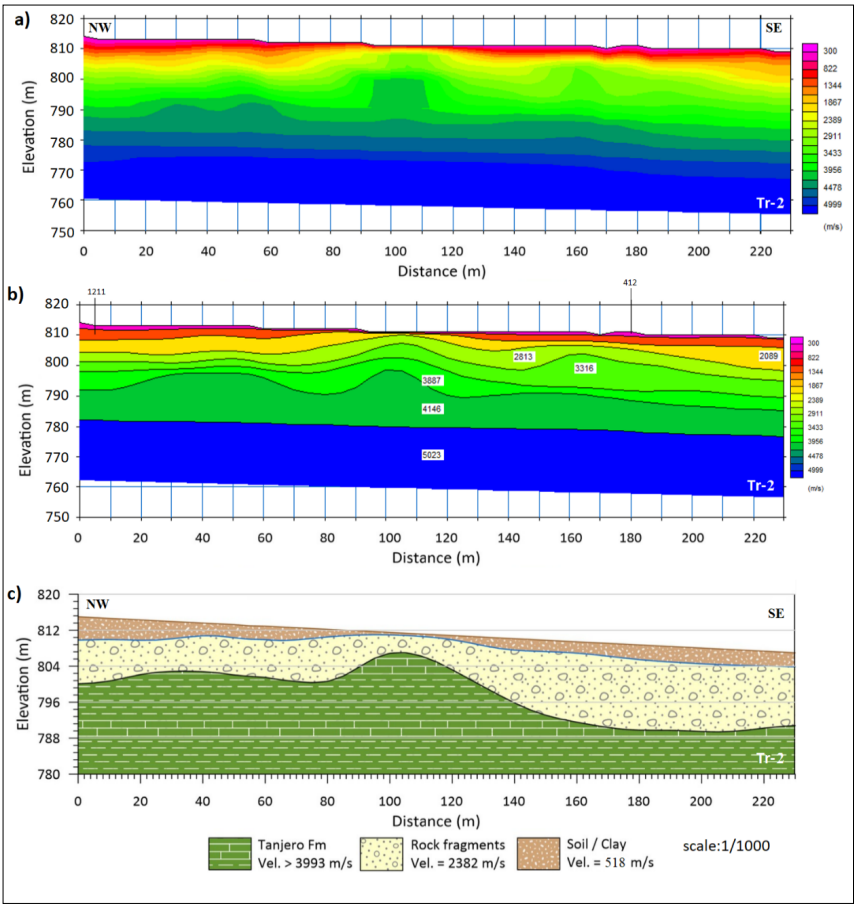

Fig. 11. SRT of traverse Tr-2; a) seismic refraction tomography (SRT) section, b) velocity model of the subsurface layers result from tomography, and c) the 2D velocity layer model and cross-section of the subsurface layers result from tomography inversion.

The **Tr-3 section** in Fig. 12 illustrates that the layers are generally parallel, with some undulations. Two uplifts are visible in the seventh sub-layer (dark green) at the top of the Tanjero formation, with elevations of 796 m occurring between distances of 50–90 m and 140–200 m. These features likely reflect the effects of erosion and weathering within the Tanjero formation.

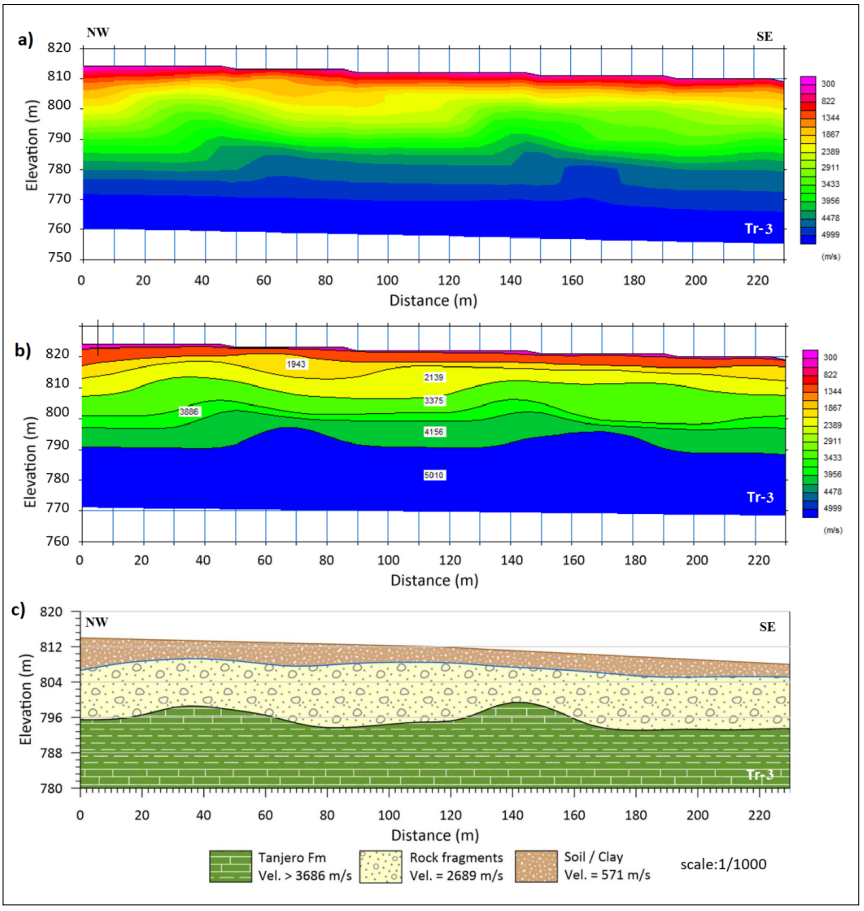

Fig. 12. SRT of traverse Tr-3; a) seismic refraction tomography (SRT) section, b) velocity model of the subsurface layers result from tomography, and c) the 2D velocity layer model and cross-section of the subsurface layers result from tomography inversion.

6.3. Traverses Tr-4 and Tr-5

Tr-4 and Tr-5, as shown in Figs. 13 and 14, respectively, exhibit similar layers and features within the aquifer layer. The seismic velocities range from 1300 to 1600 m/s, which may indicate the presence of the water table. In the third layer, two uplifts are observed in the southern parts of the traverses, located at distances between 150–190 m and 150–200 m within the silty marl bed of the Tanjero formation.

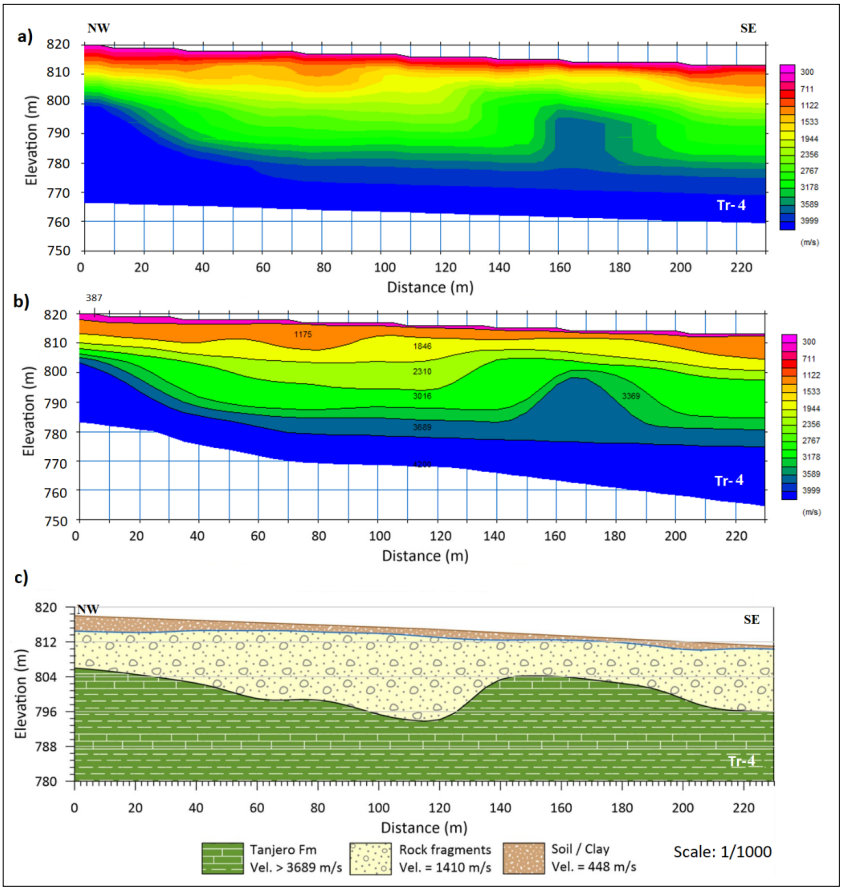

Fig. 13. SRT of traverse Tr-4; a) Seismic refraction tomography (SRT) section, b) Velocity model of the subsurface layers result from tomography, and c) the 2D Velocity layer model and cross-section of the subsurface layers result from tomography inversion.

6.4. Traverse Tr-6

The subsurface imaging along this line, which extends from northwest to southeast and runs parallel to the strike direction of the survey line, reveals small-scale (micro-features) within the third layer of the Tanjero formation, particularly around the distance of 130–160 m, as shown in (Fig. 15).

The interpretations from all SRT traverses are summarized in Table 2, as shown below.

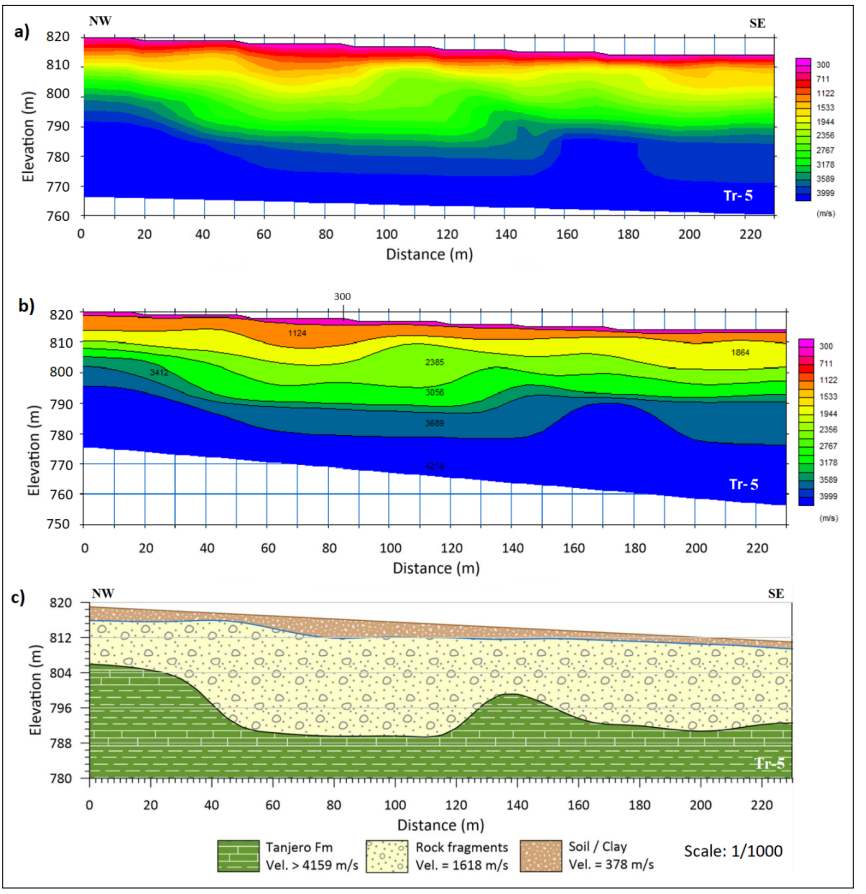

Fig. 14. SRT of traverse Tr-5; a) seismic refraction tomography (SRT) section, b) velocity model of the subsurface layers result from tomography, and c) the 2D velocity layer model and cross-section of the subsurface layers result from tomography inversion.

7. Discussion

The results indicate that a subsurface layer consists of three seismic layers with the velocity of each layer increasing with depth. The earth subsurface composition which was interpreted in relation to the information obtained from boreholes, outcrops, and the available local geology of the study site. The seismic refraction method (SRT) provides an excellent resolution of

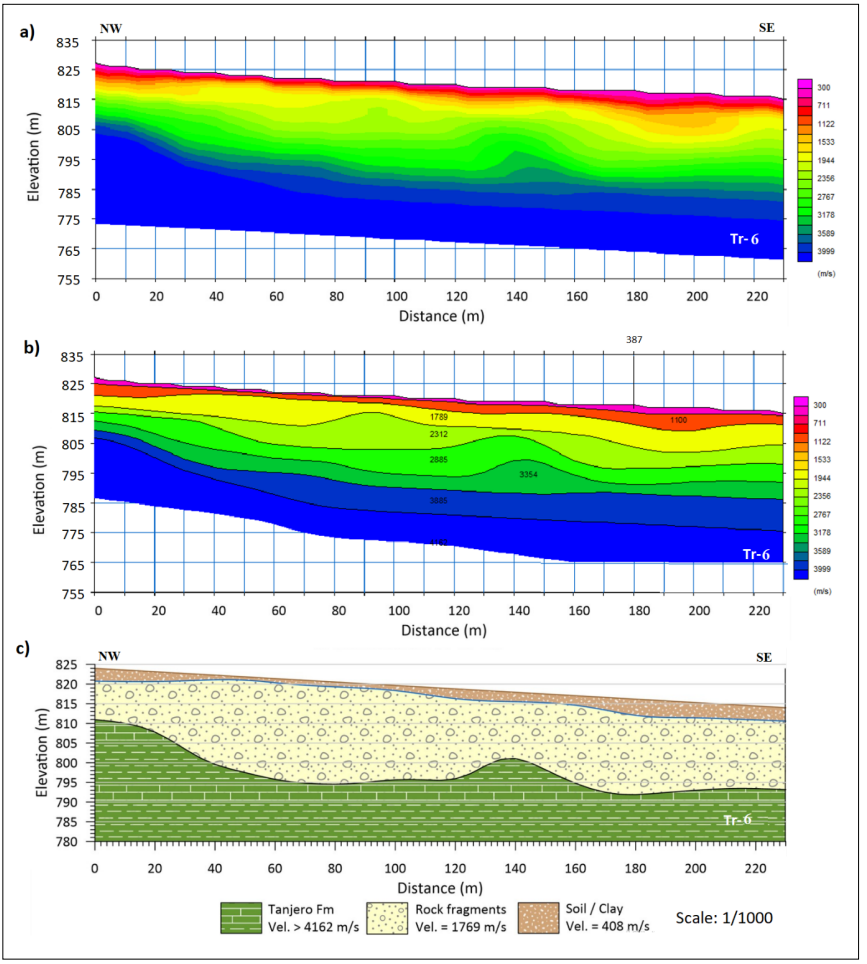

Fig. 15. SRT of traverse Tr-6; a) seismic refraction tomography (SRT) section, b) velocity model of the subsurface layers result from tomography, and c) the 2D velocity layer model and cross-section of the subsurface layers result from tomography inversion.

the bedrock boundary (layer boundary). However, it does not resolve the lithological transition at the deeper horizons due to the low amplitude of the energy source. The seismic refraction velocity varied as waves enter different geological formations, and it is considered an important method to delineate the thickness of each layer. The survey was conducted along six

Table 2. Velocities, thickness and depth for six traverses calculated by seismic refraction tomography software (automatically).

Traverses	Average layers velocities			Layers depth and thickness		
				Thicknesses		Depth of the third layer
	V_1 (m/sec)	V_2 (m/sec)	V_3 (m/sec)	Z_1 (m)	Z_2 (m)	D (m)
Tr-1	451	1896	3606	0 – 2.78	2.78 – 12.5	3 – 15.28
Tr-2	518	2383	3993	0 – 2.8	2.8 – 13.3	3 – 16.1
Tr-3	571	2689	3686	0 – 4.2	4.2 – 16.0	4 – 20.2
Tr-4	448	1410	3689	0 – 1.7	1.7 – 14.5	2 – 16.2
Tr-5	378	1618	4159	0 – 2.4	2.4 – 20.7	2 – 23.1
Tr-6	408	1769	4162	0 – 2.4	2.4 – 21.6	2 – 24.0

traverses to comprehensively cover the study area, with a geophone intervals spacing of 5 m. Each traverse extended 230 m in length, overlapping with adjacent traverses by distances ranging from 15 to 75 m to ensure continuity and data integration across the study area. This method effectively differentiated the subsurface into three distinct layers beneath the study area, successfully identifying various depressions, uplifts, and saturated zones. The shallow layer with low to moderate P-wave velocities reflects variations in grain size sediments such as sand, silt, and gravel (indicative of recent deposits), as well as elevated water content in highly saturated zones. In contrast, the high P-wave velocity layer corresponds to the middle part of the Tanjero formation, which predominantly consists of marl beds and/or highly fractured marly limestone interbedded with sandstone layers within the Tanjero formation. The results indicate that the upper boundary of the first layer exhibits a decline toward the southeastern section of the study area, attributed to processes of weathering and erosion.

8. Conclusion

This paper employs seismic refraction tomography (SRT) as the primary method for groundwater exploration in a designated area, with data collected along six traverse lines, each measuring 230 m in length. The study's findings identified three distinct layers, with seismic velocities (v_p) ranging

from 339 m/s to 583 m/s, interpreted as clay topsoil. Additionally, moderate seismic velocities between 1248 m/s and 2650 m/s indicate an unconsolidated layer comprising recent deposits of clay, sand, silt, and gravel. The results also suggest a significant groundwater potential in the study area, and the high seismic velocities (v_p) ranging from 3606 m/s to 4844 m/s indicate the presence of marly limestone bed belonging to the middle Tanjero formation, which functions as an impermeable layer.

Additionally, the results of this study correlate well with existing borehole logs in the study area. This observation further strengthens the reliability of the obtained results. Based on the 2D seismic sections analysed, it can be concluded that the recent sediments were identified in this area with thicknesses ranging from 1 to 20 m.

Acknowledgements. The authors' special thanks go to the staff of ground water directorate Sulaimani especially to the Director of the Silaimani Directorate Mr. Abbas Ali for his assistance and thanks performed to Dr. Peshawa M., Dr. Twana O. and Mr. Yassin A., for their assistance and supporting us during the preparation of the paper especially providing wells data.

References

Ali S. S., 2007: Geology and Hydrogeology of Sharazoor-Piramagrun Basin in Sulaimani Area, Northeastern Iraq. Unpublished Ph.D. Thesis, Faculty of Mining and Geology, University of Belgrade, Serbia, 330 p.

Bellen van R. C., Dunnington H. V., Wetzel R., Morton D., 1959: Lexique Stratigraphique International, Asie. Fasc. 10a, Iraq., vol. III, Paris, 336 p.

Bridle R., 2006: Plus/Minus refraction method applied to a 3D block. In: SEG Technical Program Expanded Abstracts 2006, Society of Exploration Geophysicists, 1421–1425, doi: 10.1190/1.2369786.

Chnaray M. A. H. S., 2003: Hydrogeology and Hydrochemistry of Kepran Basin Erbil-N Iraq. Unpublished Ph.D. Thesis, College of Science, University of Baghdad, 161 p.

Desper D. B., Link C. A., Nelson P. N., 2015: Accurate water-table depth estimation using seismic refraction in areas of rapidly varying subsurface conditions. Near Surf. Geophys., **13**, 5, 455–465, doi: 10.3997/1873-0604.2015039.

Dhamiry N. M, Zouaghi T., 2020: Near-surface geophysical surveys for bedrock investigation and modeling for grain silos site, Yanbu City, Western Saudi Arabia. Model. Earth Syst. Environ., **6**, 1, 51–61, doi: 10.1007/s40808-019-00654-3.

Dobrin M. B., Savit C. H., 1988: Introduction to Geophysical Prospecting, 4th ed. McGraw-Hill, New York, 867 p.

Gao Q., Shang Y., Hasan M., Jin W., Yang P., 2018: Evaluation of a Weathered Rock Aquifer Using ERT Method in South Guangdong, China. Water, **10**, 3, 293, doi:

10.3390/w10030293.

Geometrics, 2021: SeisImager/2D software, Geometrics, resources. San Jose, CA, U.S.A., available at https://geometrics.com/resources/.

Google Earth Pro, 2022: https://earth.google.com/web/@35.60519814,45.37444929,848.97739863a,16777.06932493d,35y,-0h,0t,0r.

Haeni F. P., 1986: Application of seismic-refection methods in ground water modelling studies in New England. Geophysics, **51**, 2, 236–249, doi: /10.1190/1.1442083.

Haeni F. P., 1988: Application of seismic-refraction techniques to hydrologic studies (Techniques of Water-Resources Investigations 02-D2). Report, Department of the Interior, US Geological Survey, doi: 10.3133/twri02D2.

Hassan I. O., 1998: Urban Hydrology of Erbil city region. Unpublished Ph.D. Thesis, College of Science, University of Baghdad, Geology department, 119 p.

Hasselström B., 1969: Water prospecting and rock-investigation by the seismic refraction method. Geoexploration, **7**, 2, 113–132, doi: 10.1016/0016-7142(69)90026-X.

Hodgkinson J., Brown R. J., 2005: Refraction across an angular unconformity between nonparallel TI media. Geophysics, **70**, 2, D19–D28, doi: 10.1190/1.1897028.

Janardhana Raju N., Shukla U. K., Ram P., 2011: Hydrogeochemistry for the assessment of ground water quality in Varanasi: a fast-urbanizing center in Uttar Pradesh, India. Environ. Monit. Assess., **173**, 1-4, 279–300, doi: 10.1007/s10661-010-1387-6.

Kareem A., Mustafa O., Merkel B., 2018: Geochemical and environmental investigation of the water resources of the Tanjero area, Kuristan region, Iraq. Arab. J. Geosci., **11**, 16, 461, doi: 10.1007/s12517-018-3825-7.

Karim K. H., Ali S. S., 2004: Origin of Dislocated Limestone Blocks on the Slope Side of Baranan (Zirgoez) Homocline: An Attempt to Outlook the Development of Western Part of Sharazoor Plain. J. Zankoy Sulaimani (JZS-A), **3**, 1, 5–21.

Kearey P., Brooks M., Hill I., 2002: An introduction to geophysical exploration, 3rd ed. (Vol. 4). John Wiley and Sons, Blackwell Publishing, Oxford, 288 p.

Lankston R. W., 1989: The seismic refraction method: A viable tool for mapping shallow targets into the 1990s. Geophysics, **54**, 12, 1535–1542, doi: 10.1190/1.1442621.

Loperte A., Soldovieri F., Palombo A., Santini F., Lapenna V., 2016: An integrated geophysical approach for water infiltration detection and characterization at Monte Cotugno rock-fill dam (southern Italy). Eng. Geol., **211**, 162–170, doi: 10.1016/j.enggeo.2016.07.005.

Ma'ala K. A., 2008: Geological map of the Sulaimaniyah Quadrangle. Sheet NJ-38-3, scale 1: 250,000, Iraq Geological Survey Library, Baghdad.

Mirassi S., Rahnema H., 2020: Deep cavity detection using propagation of seismic waves in homogenous half-space and layered soil media. Asian J. Civ. Eng., **21**, 8, 1431–1441, doi: 10.1007/s42107-020-00288-2.

Moore J. E., 2002: Field Hydrogeology (A Guide for Site Investigations and Report Preparation). Lewis Publishers, CRC Press, Boca Raton, 195 p.

Mota L., 1954: Determination of dips and depths of geological layers by the seismic refraction method. Geophysics, **19**, 2, 242–254, doi: 10.1190/1.1437988.

Mustafa O. M., 2006: Impact of sewage waste water on the Environment of Tanjero River and its Basin within Sulaimani city/NE-Iraq. M.Sc. Thesis, College of Science, University of Baghdad, Baghdad, 144 p.

Omar A. A., Lawa F. A., Sulaiman S. H., 2015: Tectonostratigraphic and structural imprints from balanced sections across the north-western Zagros fold-thrust belt, Kurdistan region, NE Iraq. Arab. J. Geosci., **8**, 10, 8107–8129, doi: 10.1007/s12517-014-1682-6.

Otutu O. J., 2010: Determination of ground water flow direction at Emu and Ogume Kingdoms/Nigeria. Int. J. Res. Rev. Appl. Sci., **5**, 3, 310–314.

Reynolds J. M., 2011: An introduction to applied and environmental geophysics, 2nd ed. John Wiley & Sons, 710 p.

Samyn K., Mathieu F., Bitri A., Nachbaur A., Closset L., 2014: Integrated geophysical approach in assessing karst presence and sinkhole susceptibility along flood-protection dykes of the Loire River, Orléans, France. Eng. Geol., **183**, 170–184, doi: 10.1016/j.enggeo.2014.10.013.

Sharafeldin S. M., 2008: Seismic refraction survey to characterize bedrock of dam and reservoir site, Wadi Asala, Jeddah Area, Saudi Arabia. J. Appl. Geophys. (Cairo), **7**, 1, 265–286.

Singh S., Raju N. J., Nazneen S., 2015: Environmental risk of heavy metal pollution and contamination sources using multivariate analysis in the soils of Varanasi environs, India. Environ. Monit. Assess., **187**, 6, 345, doi: 10.1007/s10661-015-4577-4.

Sissakian V. K., Fouad S. F., 2015: Geological map of Sulaimaniyah quadrangle, at scale of 1:250 000. J. Zankoy Sulaimani (JZS-A), doi: 10.13140/RG.2.1.5109.0642.

Stevanovic Z., Markovic M., 2003: Hydrogeology of Northern Iraq, Climate, Hydrology, Geomorphology and Geology, Vol. 1. Food and Agriculture Organization (FAO) coordination office for Northern Iraq, Water resources and irrigation sub sector, Ground water unit, Erbil.

Uyanık O., 2011: The porosity of saturated shallow sediments from seismic compressional and shear wave velocities. J. Appl. Geophys., **73**, 1, 16–24, doi: 10.1016/j.jappgeo.2010.11.001.

Yilmaz Ö., Eser M., Berilgen M., 2006: A case study of seismic zonation in municipal areas. Lead. Edge, **25**, 3, 319–330, doi: 10.1190/1.2184100.